Methodology for Assessing the Lithium-Sulfur Battery Degradation for Practical Applications

Knap, Vaclav; Stroe, Daniel-Ioan; Purkayastha, Rajlakshmi; Walus, Sylwia; Auger, Daniel J.; Fotouhi, Abbas; Propp, Karsten

Methodology for Assessing the Lithium-Sulfur Battery Degradation for Practical Applications

V. Knap[a], D-I. Stroe[a], R. Purkayastha[b], S. Walus[b], D. J. Auger[c], A. Fotouhi[c] and K. Propp[c]

[a] Department of Energy Technology, Aalborg University, Aalborg, 9000, Denmark
[b] Oxis Energy Ltd, Culham Science Centre, Abingdon, Oxfordshire OX14 3DB, United Kingdom
[c] Advanced Vehicle Engineering Centre, Cranfield University, Bedfordshire MK43 0AL, United Kingdom

Lithium-Sulfur (Li-S) battery is an emerging battery technology receiving growing amount of attention due to its potential high contributions of gravimetric energy density, safety and low production cost. However, there are still some obstacles preventing their swift commercialization. Li-S batteries are driven by different electrochemical processes than commonly used Lithium-ion batteries, which often results in their very different behavior. Therefore, the modelling and testing have to be adjusted to reflect this unique behavior to prevent possible biases. A methodology for a reference performance test for the Li-S batteries is proposed in this study to point out the Li-S battery features and provide guidance to users how to deal with them and possible results into standardization.

Introduction

Lithium-Sulfur (Li-S) batteries are an emerging battery technology, which is gaining interest because of its high gravimetric energy density, increased safety, and expected low production cost (1), (2), (3). Because of these features, they might become an alternative to Lithium-ion (Li-ion) batteries and replace them in various areas, such as automotive, aerospace or personal equipment. However, the swift commercialization of the Li-S batteries is still hindered by their shortcomings of low coulombic efficiency, high self-discharge, and relatively rapid capacity fade (1), (2). Nevertheless, Li-S batteries have already found areas of usefulness such as in high-altitude, long endurance unmanned aerial vehicles (4).

For product design, it is important to have a tool for comparison for the performance and the lifetime of various battery solutions. Moreover, it is required to have knowledge about the degradation of the battery in order to design safe and effective operational limits and control algorithms for the battery. Typically, the batteries accelerated degradation or lifetime tests are composed of ageing process (cycling or shelf idling) and periodical evaluation through a reference performance test (RPT). In the case of Li-ion batteries, there are several established test standards like ISO 12405-1/2 (5), (6), IEC 62660-1/2 (7), (8), which are summarized in the literature (9), (10), (11), advising how the Li-ion batteries should be tested and evaluated. Similar guidelines are required for

Li-S batteries. Unfortunately, the Li-S chemistry with its specific mechanisms prevents the direct transfer of the methodologies from the Li-ion battery world. Not respecting these specific needs would lead to biased and incomplete results about the performance-degradation of the Li-S batteries.

The primary difference between Li-ion and the Li-S batteries are their charge and discharge mechanisms. Li-ion batteries undergo an intercalation process, wherein the Li ions travel from an anode to a cathode during charging and the opposite direction during discharging. The charge and discharge processes are very symmetrical and reversible, which gives them a consistent performance (12). Contrary to the Li-ion batteries, Li-S batteries are solution-based chemistry. When the Li-S battery is fully charged the sulfur at the cathode is in the dissolved form S_8^0 or in the solid S_8^0 and dissolved form S_8^{2-} (13). During the discharge, the reduction of S_8 undergoes a set of intermediate stages. At first the long polysulfide chains of Li_2S_8 and Li_2S_6 are formed, and consequently they are reduced into the short polysulfide chains of Li_2S_4, Li_2S_2 and Li_2S. During the charge, the direction of the reactions is opposite: the long chain polysulfides are formed from the short chains. However, according to the experimental observations (14), the reaction pathways seems to be different for charge and discharge. Moreover, chemical precipitation takes place at the end of discharge for lithium sulfide and at the end of charge for sulfur. Both lithium sulfide and sulfur are insulating and insoluble. Therefore, their precipitation causes both reversible and irreversible loss of the active material depending on the cycling (2). Another inherent mechanism of Li-S batteries is the polysulfide shuttle. Due to the high solubility of the long chain polysulfides, they diffuse toward the lithium anode, where they are reduced to short chain polysulfides. Then, the reverse flux is created by the high concentration of the reduced species at the anode and the reduced short chain polysulfides diffuse back to the cathode to be oxidized again. This shuttle parasitic reaction contributes to low Coloumbic efficiency, self-discharge and irreversible capacity loss (15).

Degradation studies on Li-S batteries

Various types of studies on Li-S batteries can be found in the literature, which includes some form of degradation tests and their evaluation. They can be sorted according to their objective into three main categories:
- cell development,
- mechanism investigations,
- modelling.

Cell development

Studies focused on the cell development have usually limited scope about exploring the cells degradation. They target mainly on the comparison of cycle life of the newly developed cell to the reference cell. Sometimes, the investigations go more in depth in order to explain the source of the pro-longed life. The cells are usually cycled at only one, rarely multiple, conditions (16), (17), (18).

Mechanism investigations

The goal of studies in this category is the investigation and understanding of the degradation mechanisms and influence of various factors and conditions. As an example, the effect of binders on battery performance and degradation was investigated in (19). Brückner et al studied the influence of C-rate, amount of electrolyte and sulfur loading in (20). Furthermore, the capacity fading mechanism of the cathode was analysed in (21).

Modelling

The proposed models for the degradation of the Li-S batteries have typically one of the following roles: (i) a tool for investigation of the degradation mechanisms (22), (ii) being a part of a mechanistic model to reproduce the complex Li-S battery behavior (23) or (iii) a separate component for prediction and simulation of the capacity fade (24).

Analytical techniques

Various analytical techniques have been applied to Li-S batteries which are summarized in (2), together with their benefits and limitations. However, the scope of battery degradation testing for the practical applications in this work is limited to applicable and measureable quantities of voltage, current and temperature, which can be obtained by the use of similar test equipment as needed for the degradation tests specified for Li-ion batteries in the literature (5) ,(6), (7), (8), (10), (11).

Galvanostatic techniques. These are techniques where constant current cycling conditions are implemented i.e. full cell charge and discharge operations. These can be served as pre-conditioning cycles and can provide information about cell's charging and discharging energy, capacity and efficiencies. Furthermore, the obtained voltage profiles can be analysed for their change in the shape, or expressed as $\Delta Q/\Delta V$ vs V for an incremental capacity analysis (25), (26) or as $\Delta T/\Delta V$ vs V for thermal voltammetry analysis (27). Short current pulses applied to the battery are used to obtain the voltage response and subsequently determine the internal resistance of the battery. However, if the voltage limit is reached during the current pulse, the constant current (dis)charging mode has to switch to constant voltage mode. The user should be always careful when applying a constant charging voltage mode to the Li-S batteries due to the shuttle currents, which could result into an infinite charging of the cell and by that damaging it. The same applies for the constant current charging under specific conditions (low currents, high temperatures) where the charging time constraint should be included.

Potentiostatic techniques. Cyclic voltammetry (CV) is an often used technique for the electrochemical characterization of the Li-S cells. During the CV, the cell goes through a range of constant voltage steps and the responding current is observed. Typically, the CV for Li-S batteries shows two pairs of redox peaks, which corresponds to the voltage plateaus, obtained from the charging/discharging profiles (28). Another potentiostatic method is the direct shuttle current measurement, introduced in (15) and used for characterization and modelling in (29), in which the cell is kept at a constant voltage charging mode at the high voltage plateau until the current reaches the steady state and is matched by that the internal self-discharging shuttle current.

Electrochemical Impedance Spectroscopy (EIS). For the EIS measurements, the battery is excited by a sinusoidal current or voltage and its response on the other quantity is observed. The obtained impedance spectra are usually analysed by fitting them to an electrical circuit model, in which particular elements are assigned to the specific electrochemical processes. However, for the Li-S batteries, there is no consensus regarding the representation of the specific components (22).

Experimental tests

The 3.4 Ah Li-S long-life type cells provided by OXIS Energy were used for experiments. The measurements were performed on Digatron BTS 600 battery test station. During the experiments, cells were kept in a temperature controlled environment. Temperature of 30 °C is considered as the nominal value for comparison of the cells' performance. The nominal charging current was 0.34 A (= 0.1 C-rate) and the nominal discharging current was 0.68 A (= 0.2 C-rate). The charging cut-off limits were 2.45 V or 11 hours. The discharging cut-off limit was 1.5 V. The cycle, following these charging and discharging currents and limits, is referred as the nominal cycle.

Pre-conditioning cycles

Due to the character of the Li-S chemistry, the actual performance of the cell is highly dependent on its previous history (13), (24), which is the so-called 'cumulative history' effect. This can be illustrated on the discharge capacity test for different C-rates shown in Fig. 1. For the first cell, the discharge procedure was: (i) charging to 2.45 V/11 hours by 0.1 C-rate, (ii) discharging to 1.5 V by a specific C-rate, (iii) relaxation 15 minutes and (iv) discharge to 1.5 V by 0.2 C-rate. This procedure was repeated for various C-rates from 0.1 C-rate to 3 C-rate. As it is visible in Fig. 1(a), the discharge curves do not have a homogenous trend between each other. The discharged capacity is not always in the order of the applied current, as the cell discharged by 1.5 C-rate has lower capacity than cells discharged by 2 or 2.5 C-rates. The procedure for the second cell was modified by inserting one nominal cycle (0.1 C-rate charging, 0.2 C-rate discharging) before every charging step of the discharge capacity test procedure. The resulting discharge curves for the second cell are presented in Fig. 1(b) that shows a relatively homogenous trend for the different discharging C-rates. Therefore, a pre-conditioning cycle is required in order to obtain repeatable results at common reference state of the cells. The reason for this behavior is believed to be the precipitation of lithium sulfide. Lithium sulfide can precipitate at different rates when different discharge rates are applied. More importantly, all the lithium sulfide may not re-dissolve back on charge, leading to a temporary 'loss' of capacity. By adding an additional nominal cycle, we allow complete redissolution to occur, and essentially the cell 'resets' correctly to allow for accurate measurements.
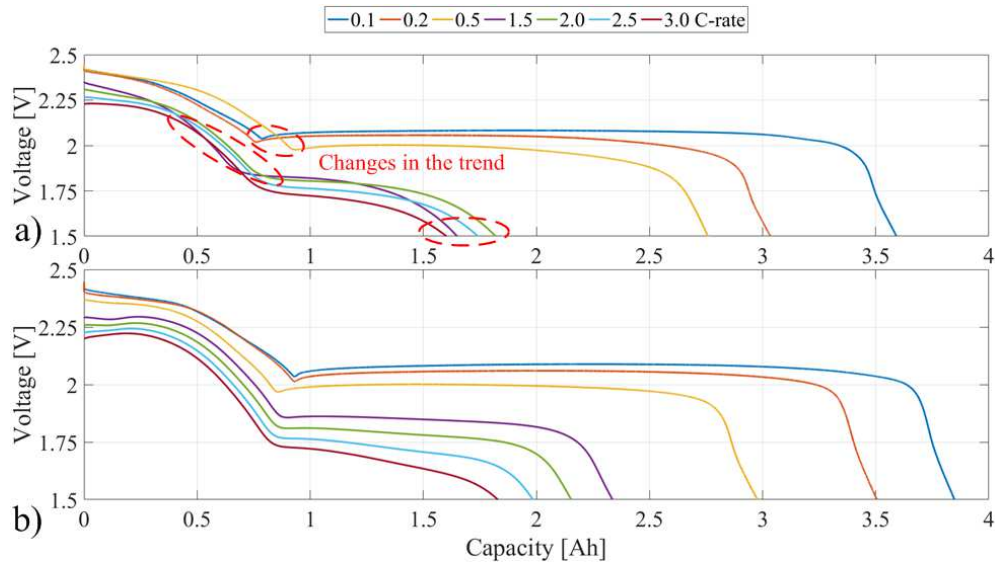
Figure 1. Voltage discharge curves for different C-rates: (a) without the pre-conditioning cycle, (b) with the pre-conditioning cycle before every charge (0.1 C-rate) and discharge (various C-rates).

The required number of pre-conditioning cycles might vary with the specific cell composition, its size and the conditions the cell is exposed to, both environmental and operational. In order to determine this number of cycles, the considered 3.4 Ah cell was exposed to 10 cycles at different specific conditions (various current and temperature), followed by 4 hours of temperature stabilization at 30 °C and subsequent 10 nominal cycles. The specific cycling conditions were selected to match the limiting conditions of the future considered degradation tests. In our case it was chosen: nominal currents at 50 °C; nominal currents at 10 °C; and 0.1 C-rate charging, 2.0 C-rate discharging currents at 30 °C. The obtained capacities from the nominal cycles at 30 °C are shown in Fig. 2, together with the capacity change between following two cycles. The capacity can be significantly different at the first cycle, but since the second cycle the changes in the capacity between the cycles are only minor. Therefore, it is concluded that only one pre-conditioning cycle is needed and the second cycle can be already used for the capacity evaluation.
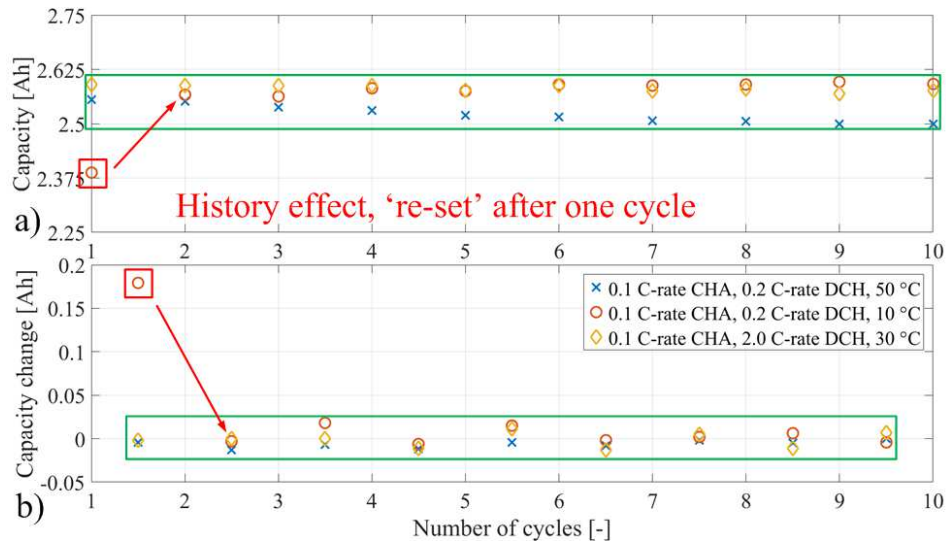
Figure 2. Evaluation of the nominal cycles at 30 °C, after cycling at different conditions; a) capacity obtained from each cycle, b) change in the capacity between the cycles.

Capacity measurement

The capacity measurement is done by using specific currents to obtain the cell capacity, energy and efficiency at the specific C-rates. For our procedure, we considered only nominal currents due to time constraints. The advantage of this consideration is that the capacity measurement and the pre-conditioning cycle are done in the same cycle. Therefore, the next step of the RPT can follow directly. The capacity obtained during the discharge is used further on for computing the SOC of the cell. The capacity measurements can be expanded by using additional C-rates; however, then adding pre-conditioning cycles before or after (due to following measurements) should be considered, together with the total time requirement for the RPT and also additional degradation of the cell during the RPT. For example, if the discharge capacity test of 1 C-rate is added, it will demand 10+1=11 hours for only the additional discharge test and also 10+5=15 hours for another pre-conditioning cycle, which will prolong the RPT by 26 hours.

Power and resistance measurement

The resistance, together with the pulse power capability, is recommended to be measured through either the hybrid pulse power characterization (HPPC) test (5), (6), (10) or through the pulse train (7), (9), (11). The HPPC test was designed for the automotive industry to evaluate the battery dynamic power capability during high pulse discharge (10 seconds, maximum discharge current), followed by a short relaxation (40 seconds) and the regenerative charge pulse (10 seconds, 0.75 of the maximum discharge current) (5). The pulse train consists of a set of charging and discharging current pulses following each other from the smallest or largest current values. The pulse is followed by another pulse with the opposite polarity in order to maintain the SOC constant. The advantage of the pulse train is that it retrieves information including the current dependence, which is especially useful when the parameter identification procedure is applied to the pulses to obtain parameter values of an electrical circuit model of the battery.

Three different values of current for charging and discharging were considered to be sufficient in order to obtain the current dependence of the battery parameters. The Li-S battery is more a high energy than a high power cell due to its relatively high resistance. Thus, even though the cell under investigation was capable of 3 C-rate continuous discharge, the total obtained capacity is significantly reduced (Fig. 1 b)) at this C-rate. Then, the discharging mode would very often be limited by voltage rather than current. Moreover, it is not a current level expected to be experienced by a single cell at the considered battery application of electric vehicles. Therefore, the current of 1 C-rate was selected as a compromise to be closer to the realistic operation scenarios. As mentioned before, the charging process of the Li-S battery is not symmetric to the discharging process, the charging pulse currents were selected to be smaller (half in our case) according to the charging capability of the cell. Finally the applied currents were 0.1, 0.2 and 0.5 C-rate for charge pulses and 0.2, 0.5 and 1 C-rate for discharge pulses.

The relaxation period between the pulses for the Li-ion batteries is recommended to be 10 minutes (7), unless the cell temperature is still higher than 2 °C of target test temperature, then the cell can be cooled down or the relaxation period can be prolonged. For the Li-S battery, we have first extended the relaxation period to 15 minutes and performed the preliminary pulse train test from 90 % SOC to 10 % SOC at 25 °C. For obtaining the necessary relaxation time between the pulses, the following assumption was taken in order to compute the settling time: the system is sufficiently relaxed when the voltage reaches 95 % of a quasi-steady state voltage value (at 15 minutes of the relaxation after the pulse) from the initial voltage drop value. Only the worst case of the current was considered, i.e. 0.5 C-rate for charging and 1.0 C-rate for discharging. The obtained settling time values are summarized in Table I. At very high SOC, the polysulfide shuttle changes the character of the recovery voltage and therefore, the settling time at 90 % of SOC varies significantly from the other SOC levels. The average values for the interval from 80 to 10 % SOC were computed to be 470 seconds = 7.83 minutes for 1.0 C-rate discharge pulses and 248 seconds = 4.13 minutes for 0.5 C-rate charge pulses. Rounding the numbers up to 10 and 5 minutes for discharging and charging consequently provides a margin to ensure that the cell should be sufficiently relaxed and the values should be valid also for the SOC levels at the neighboring temperature levels (such as 20 or 30 °C) with a lower rate of the polysulfide shuttle.

TABLE I. **Settling time after pulses at various SOC levels.**

SOC [%]	90	80	70	60	50	40	30	20	10	Avg
Pulse current				Settling time [seconds]						
1 C-rate DCH	108	480	586	562	569	500	452	311	297	470
0.5 C-rate CHA	622	430	89	200	353	179	316	244	173	248

When 10 and 5 minutes relaxation periods between pulses were applied, there has been observed a steep voltage drop at 100 and 90 % SOC due to the prevalence of the polysulfide shuttle. Moreover, the 'equilibrium point' (=the peak point between voltage recovery after discharge and voltage decay due to the self-discharge) was present relatively early. Therefore, the relaxation periods can be much shorter, which is also preferable due to smaller shift of the SOC caused by the self-discharge. It has been assumed that only half of the relaxation periods used for other SOC levels (5 minutes for discharging and 2.5 minutes for charging pulses) is sufficient for 90 % SOC and quarter

of it (2.5 minutes for discharging and 1.25 minutes for charging pulses) is enough for 100 % SOC.

After the discharging steps between different SOC levels and before the first pulse, there is a requirement for an additional relaxation time to allow the cell to reach an equilibrium state. However, for some SOC levels that would mean a relaxation in range of hours, which would considerably pro-long the overall test procedure. Therefore, a 30 minutes long relaxation period is considered sufficient to reach a quasi-equilibrium state for the cell before the pulse train procedure. The applied pulse train for 0 to 80 % SOC is illustrated in Fig. 3. Again, due to the self-discharge at higher SOC levels, the relaxation is shortened to 15 minutes at 90 % SOC and it is only 1.5 minutes at 100 % SOC.
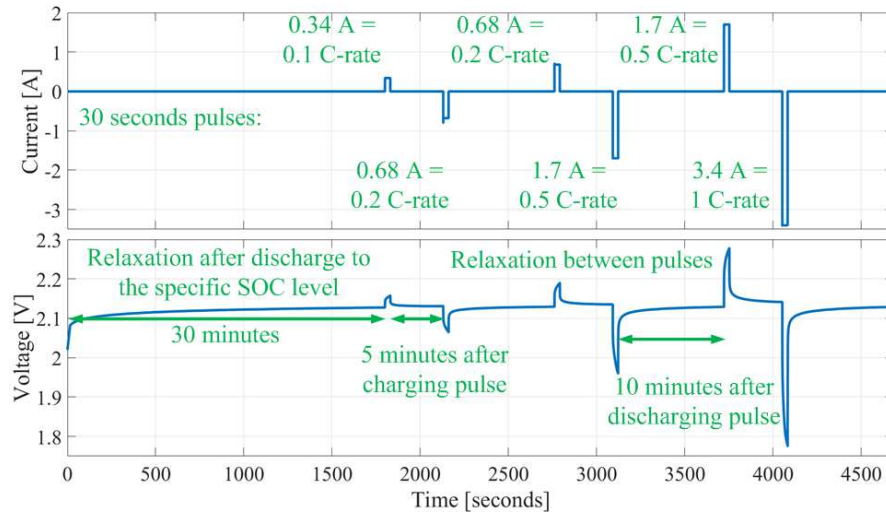

Figure 3. Illustration of the applied pulse train procedure for SOC levels between 0 and 80 % SOC.

The last step is to correctly determine the discharging step between the SOC levels. Due to inequality between the charging and discharging pulses, the SOC shifts down by 0.75 % per pulse train, except at 100 % SOC, where 0.5 C-rate charging pulse is omitted, as the limiting voltage is already reached by 0.2 C-rate charging pulse; and therefore the SOC shift down is by 1.2 %. The discharging steps should be adjusted to account for this SOC shift. Moreover, the approximate self-discharge can be estimated by the Li-S self-discharge model (29) with a consideration of a fresh cell with 3.4 Ah capacity. The pulse train procedure at 100 % lasts 14 minutes (1.5 minutes relaxation period before the first pulse, 2*0.5 minutes charging pulses, 3*0.5 minutes discharging pulses, 2*1.25 minutes relaxation after charging pulses and 3*2.5 minutes relaxation after discharging pulses), which results into loss of 0.78 % SOC. Therefore, immediately after the pulse train at 100 % SOC level, the actual SOC would be rather 98 %. So the discharge to 90 % SOC level can be reduced down to step of 7.5 % SOC, to account for the previously described occurrences and for the self-discharge during this discharging step. A similar procedure can be applied to compensate for the self-discharge during the pulse train at 90 % SOC; however, its effect is under 1 % SOC and it is considered insignificant to be dealt with. The last effect, which can be considered for adjustment of the discharging steps between SOC levels, is the charge recovery effect (30). As the cell is relaxed between the discharging steps, its effective capacity is higher than during the continuous discharge.

Therefore, the discharging step between 10 % and 0 % SOC should be controlled rather by discharging to cut-off voltage limit of 1.5 V than controlled by the amount of discharged SOC, in order to bring the cell to the state when is actually no charge available. The summary of different settings according to SOC levels are presented in Table II.

TABLE II. **Specifications for pulse train procedure at various SOC levels.**

SOC level [%]	100	90	80 - 10	0
Discharging step to the SOC level	-	7.5 %	9.25 %	to 1.5 V
Relaxation before the pulse train [min]	1.5	15	30	30
Relaxation after charging pulse [min]	1.25	2.5	5	5
Relaxation after discharging pulse [min]	2.5	5	10	10

Shuttle current measurement

The polysulfide shuttle is a unique mechanism, which has no equivalent within classical Li-ion batteries; nevertheless, for Li-S batteries it is very important, as it is related to the self-discharge, degradation, columbic efficiency and possibly also to the safety. Moy et al (15) introduced the methodology for the measurement of the polysulfide shuttle current, which is based on constant voltage charging until the external current reaches a steady-state and which indicates that it has equalized with the internal shuttle current.

The procedure follows downward SOC direction, so at first the cell has to be charged. Then the cell is discharged to the target SOC level and it is relaxed until the voltage equilibrium is reached. The voltage equilibrium is understood to be the peak voltage value, which occurs between increasing voltage in the recovery period immediately after the interruption of discharging current; and decreasing voltage due to self-discharge in pro-longed relaxation. In practice, the voltage equilibrium can be detected by the voltage falling under the threshold from the maximum voltage value, where the threshold is set with respect to the measurement accuracy and noise. When the threshold is crossed, this voltage value is used as the limit for constant voltage charging, which lasts until the current reaches steady-state value, typically limited by time. Afterwards, it is followed by the discharging to the next investigated SOC level.

The shuttle current measurement to 3.4 Ah Li-S cells was already applied in (29). From where it is known that two hours period of constant voltage charging is enough for these cells to reach steady-state. Moreover, the voltage threshold applied in Digatron BTS 600 battery test station is 0.6 mV. It is considered that three different SOC levels for the shuttle current measurement should be enough, together with the fourth level with known zero current, to use the results for the fitting and deriving a relation of the shuttle current against SOC or open circuit voltage. As the target SOC levels, 98%, 94%, and 88% of SOC were considered.

Summary

The content of the RPT for the Li-S batteries is shown in Fig. 4. The specific steps were adjusted according to needs of the specific cell type, in our case 3.4 Ah Li-S pouch cell from OXIS Energy. It has been found that 4 hours temperature stabilization and one

pre-conditioning cycle (0.1 C-rate charging, 0.2 C-rate discharging) are sufficient to 'reset' the cells history and obtain comparable results from the following RPT procedure after exposing the cell to cycling at three extreme conditions. The capacity measurement is performed only for the nominal currents of 0.1 C-rate for charging and 0.2 C-rate for discharging, which allows to move to the next step of power and resistance measurement without additional pre-conditioning cycle inbetween. The power and resistance measurement is done by the pulse train starting from 100 % SOC and continue down to 0 % by the steps of 10 %. The pulses are assymetric for charging and discharging. The additional step of the RPT for the Li-S batteries is the shuttle current measurement, which allows to quantify the shuttle in a straightforward way and by that provide information about the self-discharge and the degradation rate. The voltage profile of the proposed RPT procedure is shown in Fig. 5.

Typical RPT procedure at Li-ion batteries:

- Pre-conditioning cycles
- Capacity measurement
- Power and resistance measurement

Proposed RPT procedure for Li-S batteries:

- Pre-conditioning cycles
- Capacity test
- Power and resistance measurement
- Shuttle current measurement

Figure 4. Content of the RPT for Li-ion and Li-S batteries.
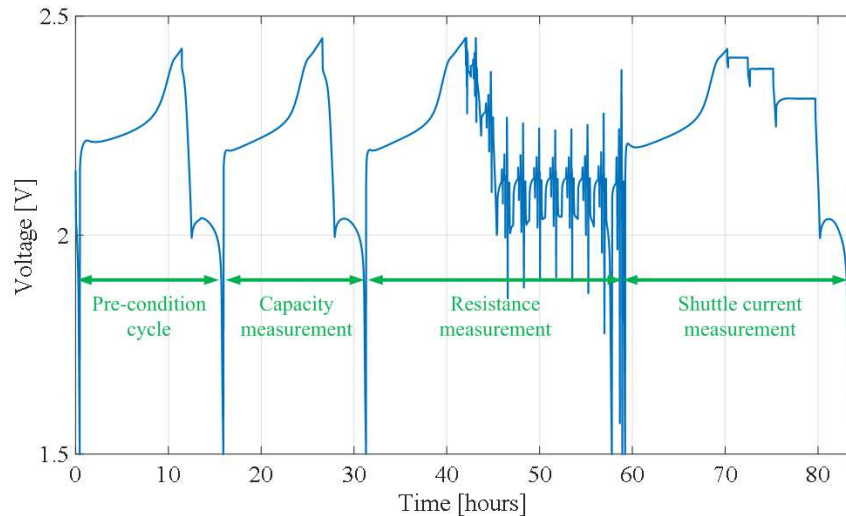

Figure 5. Illustration of the complete RPT procedure for the Li-S batteries.

Conclusions

The Li-S batteries with their unique behavior require specific approaches, where every method applied for Li-ion batteries should be reconsidered, if it is suitable or not. Often, it is not possible to directly take proven approaches from the world of Li-ion batteries, such as modelling and testing, and apply them to the Li-S batteries without introducing a bias or significant loss of accuracy. Therefore, a RPT procedure for the Li-S batteries is proposed in this manuscript, to bring attention to the specific issues and differences of this type of batteries and to provide guidance to other users. The RPT is typically used to evaluate the performance of the batteries related to the practical applications and often it is applied to identify influence of ageing at different conditions.

Acknowledgments

References

1. D. Bresser, S. Passerini, and B. Scrosati, *Chem. Commun.*, **49**, 10545–10562 (2013).
2. M. Wild, L. O'Neill, T. Zhang, R. Purkayastha, G. Minton, M. Marinescu, and G. J. Offer, *Energy Environ. Sci.* (2015).
3. I. a. Hunt, Y. Patel, M. Szczygielski, L. Kabacik, and G. J. Offer, *J. Energy Storage*, **2**, 25–29 (2015).
4. G. Xian-Zhong, H. Zhong-Xi, G. Zheng, Z. Xiong-Feng, L. Jian-Xia, and C. Xiao-Qian, *Aircr. Eng. Aerosp. Technol.*, **85**, 293–303 (2013).
5. *ISO 12405-1:2011 Electrically propelled road vehicles – Test specification for lithium-ion traction battery packs and systems – Part 1: High-power applications*, (2011).
6. *ISO 12405-2:2012 Electrically propelled road vehicles – Test specification for lithium-ion traction battery packs and systems – Part 2: High-energy applications*, (2012).
7. *IEC 62660-1: Electrically propelled road vehicles - Test specification for lithium-ion traction battery packs and systems - Part 1: High power applications*, (2011).
8. *IEC 62660-2: Secondary batteries for the propulsion of electric road vehicles - Part 2: Reliability and abuse testing for lithium-ion cells*, (2011).
9. G. Mulder, N. Omar, S. Pauwels, F. Leemans, B. Verbrugge, W. De Nijs, P. Van Den Bossche, D. Six, and J. Van Mierlo, *J. Power Sources*, **196**, 10079–10087 (2011).
10. The Idaho National Laboratory, *Battery Test Manual For Plug-In Hybrid Electric Vehicles*, (2012).
11. D.-I. Stroe, M. Swierczynski, A.-I. Stan, R. Teodorescu, and S. J. Andreasen, *IEEE Trans. Ind. Appl.*, **50**, 4006–4017 (2014).
12. H. He, B. Liu, A. Abouimrane, Y. Ren, Y. Liu, Q. Liu, and Z.-S. Chao, *J. Electrochem. Soc.*, **162**, A2195–A2200 (2015).
13. M. Marinescu, T. Zhang, and G. J. Offer, *Phys. Chem. Chem. Phys.* (2015).

14. Q. Wang, J. Zheng, E. Walter, H. Pan, D. Lv, P. Zuo, H. Chen, Z. D. Deng, B. Y. Liaw, X. Yu, X. Yang, J.-G. Zhang, J. Liu, and J. Xiao, *J. Electrochem. Soc.*, **162**, A474–A478 (2015).

15. D. Moy, a. Manivannan, and S. R. Narayanan, *J. Electrochem. Soc.*, **162**, A1–A7 (2014).

16. M. R. Kaiser, J. Wang, X. Liang, H.-K. Liu, and S.-X. Dou, *J. Power Sources*, **279**, 231–237 (2015).

17. H. Yao, G. Zheng, P.-C. Hsu, D. Kong, J. J. Cha, W. Li, Z. W. Seh, M. T. McDowell, K. Yan, Z. Liang, V. K. Narasimhan, and Y. Cui, *Nat. Commun.*, **5**, 3943 (2014).

18. X. Li, M. Rao, D. Chen, H. Lin, Y. Liu, Y. Liao, L. Xing, and W. Li, *Electrochim. Acta*, **166**, 93–99 (2015).

19. E. Peled, M. Goor, I. Schektman, T. Mukra, Y. Shoval, and D. Golodnitsky, *J. Electrochem. Soc.*, **164**, A5001–A5007 (2017).

20. J. Brückner, S. Thieme, H. T. Grossmann, S. Dörfler, H. Althues, and S. Kaskel, *J. Power Sources*, **268**, 82–87 (2014).

21. Y. Diao, K. Xie, S. Xiong, and X. Hong, *J. Electrochem. Soc.*, **159**, A1816–A1821 (2012).

22. Z. Deng, Z. Zhang, Y. Lai, J. Liu, J. Li, and Y. Liu, *J. Electrochem. Soc.*, **160**, A553–A558 (2013).

23. A. F. Hofmann, D. N. Fronczek, and W. G. Bessler, *J. Power Sources*, **259**, 300–310 (2014).

24. S. Risse, S. Angioletti-Uberti, J. Dzubiella, and M. Ballauff, *J. Power Sources*, **267**, 648–654 (2014).

25. M. Dubarry, V. Svoboda, R. Hwu, and B. Yann Liaw, *Electrochem. Solid-State Lett.*, **9**, A454–A457 (2006).

26. V. Knap, K. Theodoros, R. Purkayastha, B. Szymon, D.-I. Stroe, E. Schaltz, and R. Teodorescu, *Transferring the Incremental Capacity Analysis to Lithium-Sulfur Batteries*, (2017).

27. B. Wu, V. Yufit, Y. Merla, R. F. Martinez-Botas, N. P. Brandon, and G. J. Offer, *J. Power Sources*, **273**, 495–501 (2015).

28. Y.-X. Yin, S. Xin, Y.-G. Guo, and L.-J. Wan, *Angew. Chemie Int. Ed.*, **52**, 13186–13200 (2013).

29. V. Knap, D. I. Stroe, M. Swierczynski, R. Purkayastha, K. Propp, R. Teodorescu, and E. Schaltz, *J. Power Sources*, **336**, 325–331 (2016).

30. V. Knap, T. Zhang, D. I. Stroe, E. Schaltz, R. Teodorescu, and K. Propp, *ECS Trans.*, **74**, 95–100 (2016).